Multi-Band Image Classification Using Klt and Fractal Classifier

[*]Laith Abdul Aziz Al-Ani and [**]Mohammed Sahib Mahdi Al-Taei
[*]Department of Physics , College of Science , Al-Nahrain University.
[**]Department of Computer Science, College of Science, Al-Nahrain University.

Abstract

In this paper, a multi-spectral satellite image of known training areas taken in six bands is used. The adopted classification method suggests transforming the six bands into new six other bands using KL transform. The information of the image is redistributed to be concentrated in the first transformed band, the information is decreases gradually in the remaining bands. Thus, the first three transformed bands that carried most of image features can only be used to achieve more accurate classification. The first chosen band was partitioned into blocks by quadtree method. Then the most popular fractal feature namely lacunarity was estimated for each block to classify them. The results showed six classes, which were greatly identifying the training areas existing in the image. The classification score was found about 91% when the contribution weight of the first band is 90%. This score increases lightly by increasing the weight of contributing the first band.

Keywords: Image classification, KL transforms, Fractals, multi-bands images.

1. Introduction

The Landsat series of satellites (starting with the Earth Resources Technology Satellites) have acquired millions of imagery since 1972 and is the longest continuous strategy for acquiring imagery of the Earth's biosphere from space. A single scene acquired by the Landsat earth resource satellite system using the Thematic Mapper (TM) instrument typically covers185 *km* x 185 *km*. The image consists of about 40 million pixels, six spectral bands at 30 *m* resolution (120 *m* for the thermal band) and 8-bit dynamic range. One Landsat TM scene has a file size of over 300 *MB*. Each pixel covers 0.09 hectares on the ground [1].

A multispectral (6 bands) landsat TM mosaic of the conterminous United States (US) at 30 *m* resolution, requires 428 scenes (single coverage) and results in an image with dimension of 218,000 x 95,000 pixels and uses 160 *GB* of storage space at multiple resolutions. The conterminous US Landsat TM mosaic was created by the NASA Jet Propulsion Laboratory, and is certainly one of the largest seamless single images produced to date [2].

Many applications based on using Landsat imagery in a quantitative fashion require classification of image pixels into a number of relevant categories or distinguishable classes. Landsat imagery has been used in a wide range of domains including understanding seasonal and annual cycles of the Earth's environment for global change research, agricultural land use and crop monitoring, forest inventory management, geological and mineral surveys, water resource estimates, and coastal zone appraisal [3]. Specific applications include mapping statewide forest cover, deforestation, terrain, soil moisture, mining activity, land reclamation, water quality, population change, urbanization impact, commercial site location, etc. Classification is a means of complementing retrieval. Several methods have been proposed for classifying block of image by clustering based on their features and representing the classification results by means visualization techniques. The static template method (called Class Models) based on the relationship between different areas in an image in terms of their intensity features is applied to classify the nature photographs [4].

Fractal geometry provides a suitable satellite image classification framework by studying the nature irregularity shapes since it allows to easily describing such fractal images. The fractal geometry can recognize small segment of image that characterized by its spectral uniformity, this necessitate first to segment the image before the classification [5]. The main characteristics of fractal images are that they are continuous but not differentiable and that they show a fine detailed at any arbitrarily small scale. A fundamental concept of fractal geometry is the

fractal dimension, at any fractal application, one can use the fractal dimension as a recognizable fractal feature because it is a measure of complexity in fractal patterns, the higher fractal dimension the more complex the fractal pattern [6]. Because the fractal dimension F takes non-integer (i.e., $2<F<3$) number it is difficult to recognize plenty of classes well. Mandelbrot suggest another fractal measure call it lacunarity to handle the case of sharing two different classes with same fractal dimension [6]. Later, lacunarity is used as a similarity measure to distinguish two fractal sub-images. Lacunarity is a set of points (curve) computed by the box counting method, which is the same method of computing the fractal dimension. Box counting method is a common and accurate one for computing the fractal dimension and the lacunarity, but it has some of complexity [7].

2- Theoretical Framework

Image partitioning using quadtree method needs to store 5 pointers, one for the parent subimage and one for each of its 4 node subimages as shown in Fig.(1-a). The quadtree codes for a square $2^k \times 2^k$ pixel block made by *n-k* successive subdivision into quadrants consists of *n–k* quaternary digits, where the i^{th} digits is 0,1,2 or 3 according to the i^{th} subdivision was into the *NW*, *NE*, *SW*, or *SE* quadrant, followed by *k* zeros. The number *k*, is called the *order* of the subimage, is then applied to the code as a second integer. In a linear quadtree of Fig. (1-b), only the black nodes are stored. Each one contains a quaternary code and a single pointer to the next node (the node are stored as a linked list to enable quick insertion and deletion and are also stored according to their codes for conversion to a sorted array should searches become necessary). The purpose of padding the *n-k* digits on the right with *k* zeros is to keep them from being implicitly padded of the left, which would allow different subimages of the same picture to have the same code. For example, without the padding the codes 003, 030, and 300 all would be stored as 3 and interpreted as 003. With the padding, the code is the same for a subimage as for its *NW* pixel; they are distinguished by their order [8].

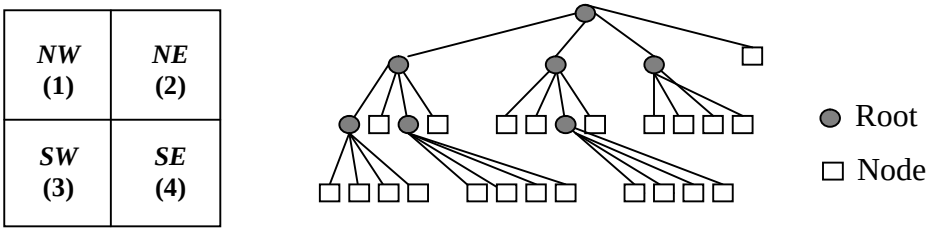

(a) **(b)**

Fig. (1) Quadtree segmentation.

In the current research, the partitioning condition of the quadtree method is related to uniformity of each block. The quadtree of a $2^n \times 2^n$ picture is a rooted directed tree generated by the recursive a square subimage of the image, with the root representing whole image. If the subimage represented by a given node does not satisfy the condition then the node is a leaf of that root; otherwise the subimage is divided into 4 equal sons [9].

The fractal dimension F of a set S contained in R^n is estimated for B^2 subimage (leaf) $B>0$, by assuming $N_B(S)$ is the minimum number of η-dimensional cubes of side B needed to cover S. If there is a number F so that [10];

$$N_B(S) \approx 1/B^F \quad \text{as } B \to 0 \quad \ldots\ldots\ldots\ldots\ldots (1)$$

Note that the fractal dimension is F if there is some positive constant C [8],

$$\lim_{B\to 0} \frac{N_B(S)}{1/S^F} = C \quad \ldots\ldots\ldots\ldots\ldots\ldots\ldots\ldots\ldots (2)$$

Since both sides of the equation above are positive, it will still hold if one takes the logarithm of both sides to obtain [8];

$$\lim_{B\to 0}(\ln(N_B(S) + F \times \ln(S))) = \ln(C) \quad \ldots\ldots\ldots (3)$$

Solving for F gives

$$F = \lim_{B\to 0} \frac{\ln(C) - \ln(N_B(S))}{\ln(B)}$$

$$F = -\lim_{B\to 0}\frac{\ln(N_B(S))}{\ln(B)} \quad \text{.....(4)}$$

Note that *ln*(*C*) drops out, because it is constant while the denominator becomes infinite as $B \to 0$. Also, since $0 < B < 1$, *ln*(*B*) is negative, so *F* is positive as one would expect. The lacunarity is now given as [8];

$$L = E\left[\left(\frac{M}{E(M)} - 1\right)^2\right] \quad \text{.....(5)}$$

Where, *L* is the lacunarity, *E*(*M*) is the expectation value, and *M* is the mass of the intersection of the considered set with a box of size *B*. This definition measures the discrepancy between the actual mass and the expected mass. Besides, since *M* depends on *B* we have that lacunarity depends on *B*, too [8,10]. For each segmented block, the lacunarity is assumed to be a classifier parameter. So, it is expected the different neighbor blocks lead to make their extracted features have recognizability among other blocks.

3. Materials and Methods

The material image consists of six TM-multispectral bands of Ramadi sense image shown in Fig.(2). According to literatures, the six bands of the used image possess six training areas, they are; desert, urban, tree, vegetation, shallow water, and deep water. The classification of the image needs first to preprocess these six bands in order to appear the features that recognize each class. This is carried out by transforming the image into another domain, where the embedded features of the original image can be resolved in the new six transformed bands. Only the most informatics band is partitioned by quadtree method.

The fractal feature was then estimated for each block, which help the classifier to guide the block into its corresponding class. The block diagram shown in Fig.(3) presents the processing series done for each band in the image, more details about each process is mentioned in the section of implementation and results:

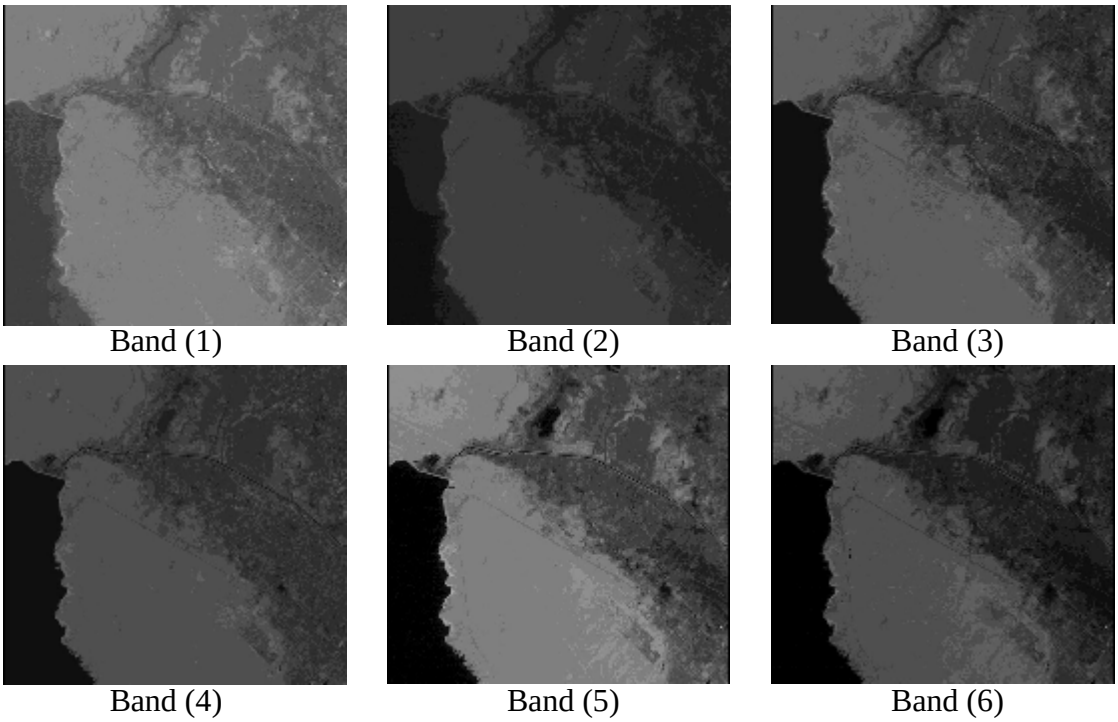

Fig. (2) The six bands of Ramadi sense image.

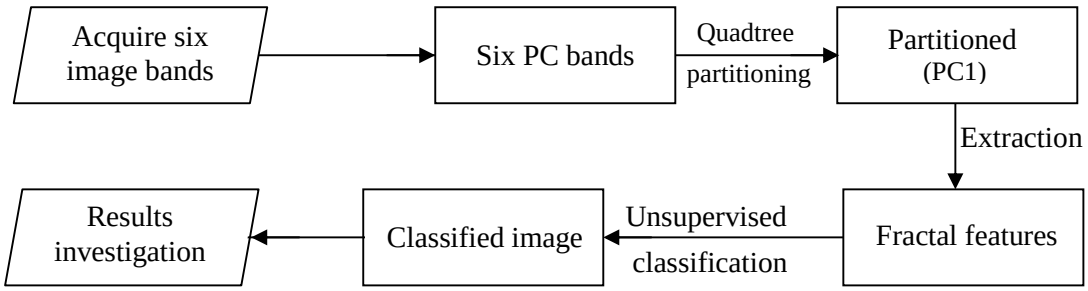

Fig. (3) Block diagram shows the processing series.

4. Implementation and Results

The following subsections include an explanation about how implement the proposed method and displays the results for each processing stage. These stages do not walk through the planned traces exactly since the natural images carried more details and need to more treatment. The processing of classification and the treatment are offered below in details.

4.1 KL Transformation

The KL transform is used to get six new bands carried the principal components (PC), shown in Fig.(4). The comparison between the output PCs (see Fig. (4)) and the input original bands (see Fig. (3)) shows that the first PC contains greater contrast since it clearly appear the fine details of the image. The computations refer to that the first three PCs possess 98% from the information of the original image, and the remaining percentage (i.e., 2%) is distributing on the latter three transformed PCs decently. This paved the way to utilize the more informatic first PC to be partitioned by the quadtree into unequally square blocks.

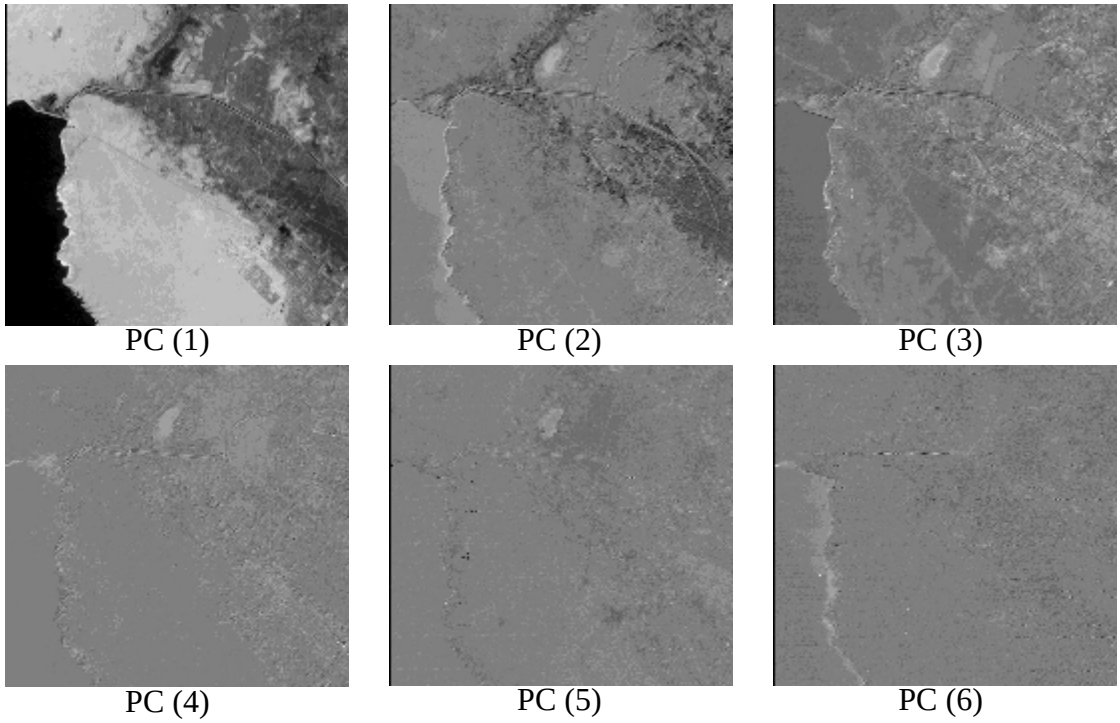

Fig. (4) Six KL transformed bands (PCs) of Ramadi sense image.

4.2 Quadtree Partitioning

The partitioning process utilizes the spectral variety condition to partition the image into blocks. According to that, the first PC was partitioned into many blocks depending on the variety of the local gray in each block. These conditions depend basically on the local mean and standard deviation of both the parent and its four nodes. The results of the partitioning gave a convincing result about the splitting conditions. Algorithm (1) presents the application of the quadtree method on the first transformed bands of Ramadi image, whereas the partitioned PC1 is shown in Fig.(5):

Begin
M_G= Global mean of the image
S_G= Global standard deviation of the image
Determine *Fraction* and *Accepted ratio*
Do
Do for each block
M_B=mean of current block (i.e. node)
g= gray of current pixel
if $|g-M_B| > Fraction*S_G$ ***then*** $n=n+1$
Loop
If $n<$*Accepted ratio* ***then***
Split the root into four quadrants
Get next root
Loop until there is no splitting
End

Algorithm (1) Quadtree segmentation (e.g., Fraction=0.1;Accepted ratio=0.2).

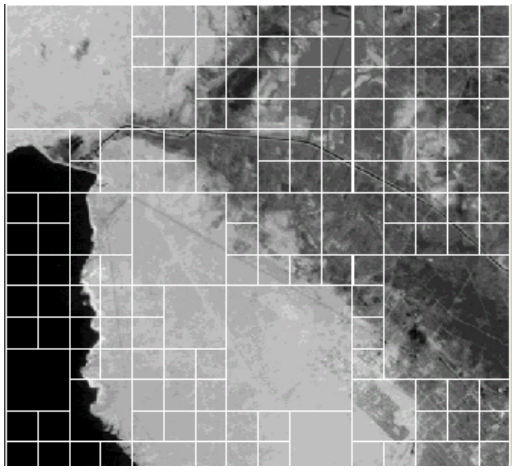

Fig. (5) The segmented PC1 image using quadtree method.

4.3 Feature Extraction

The fractal classification parameter "lacunarity" is extracted for each segmented block by using the box counting. The blocks that have different spectral details were giving different shapes of lacunarity curve and vice versa. The height of lacunarity curve is found greatly related to brightness of current block, which may affect the lacunarities comparison. The increase of brightness causes a shift in the lacunarity curve upward, while its decrease causes a shift in the lacunarity curve downward. In both cases the lacunarity shape was conserved. It is noticed that the shape of the lacunarity related by the amount of the roughness of the spectral details in each block. The variation of the lacunarity height with brightness may confuse the result of comparison between any two lacunarities belong to different classes. This problem was bypassed by normalizing all the resulting lacunarity curves before comparing them with others, this credit to give an actual indication about the comparison decision.

4.4 Unsupervised Classification

Unsupervised classification is process of assigning the blocks of image into six classes according to the similarity of the lacunarity shapes. Each group of similar lacunarities is considered to be a class. This process is carried out through the following three steps;

1. The three adopted PCs of the image have different details comparing with each other. Therefore, the ith band should be contributed by a weight (W_i) is proportional to its carried information. The contribution weight is a percent computed depending on its gray variance as follows;

$$W_i = \frac{V_i}{V_T} \times 100\% \quad ,i = 1,2,or\ 3 \quad \text{.....} (5)$$

where, V_i is the gray variance of the i^{th} PC band, V_T is the total sum of variance of the three PC bands. The computations show that W_1=90%, W_2=7%, and W_3=3%.

2. The comparison between the lacunarity shapes of current block with that of the other block for each band is computed depending on suggested similarity measure. The similarity measure (S_{ij}) is computed with regarding the contribution weights of each band as follows;

$$S_{ij} = 1 - \left(W_i \times \sum_{k=1}^{B} \left| L_{ij} - L_{ik} \right| \right) \quad (\forall\ j \neq k)$$

..... (6)

where, i is pointer refers to the current PC band, j and k are pointers refer to the j^{th} and k^{th} block respectively, B is the number of blocks, L_{ij} and L_{ik} are the lacunarities of the j^{th} and k^{th} block existing in i^{th} PC band. The resulting similarity measure used to distinguish between two lacunarity curves; when $S_{ij} = 1$ the two compared lacunarities are absolutely similar to each other, and when $S_{ij} = 0$ they are absolutely different, whereas the fractional number indicates the similarity in between. Practically, one can notes that the resulted lacunarity shapes do not have exact identification with each other, but their general behavior is seen to be similar. The similarity measure less than 0.6 leads to different classes, other wise leads to similar classes.

3. Current step necessitates to build a classifier routine goes to divide the lacunarities into six groups according to S_{ij} between them. Each group represents a class. The strategy of the classifier is to put all the lacunarities and its S_{ij} in buffer, and then hold one of them to search for all of its similar lacunarities (i.e., to find greatest $S_{ij} : 0 \le S_{ij} \le 1$). The detected similar lacunarity is registered in a specific record and removed from the buffer. This process is repeated on the remaining lacunarities till the last block.

4.5 Results Investigation

The lacunarity gave encouraging unsupervised classification results, where each class of image has a relatively different shape of lacunarity. The total classification percentage was 91% when the contribution weight of the adopted three PC bands are 90% for the first, 7% for the second, and 3% for the third band. A presentation of classification result corresponding to the segmented PC bands (see Fig.(5)) is pictured in Fig.(6), whereas Fig.(7) displays the shapes of the normalized lacunarity curve that characterizes each.class.

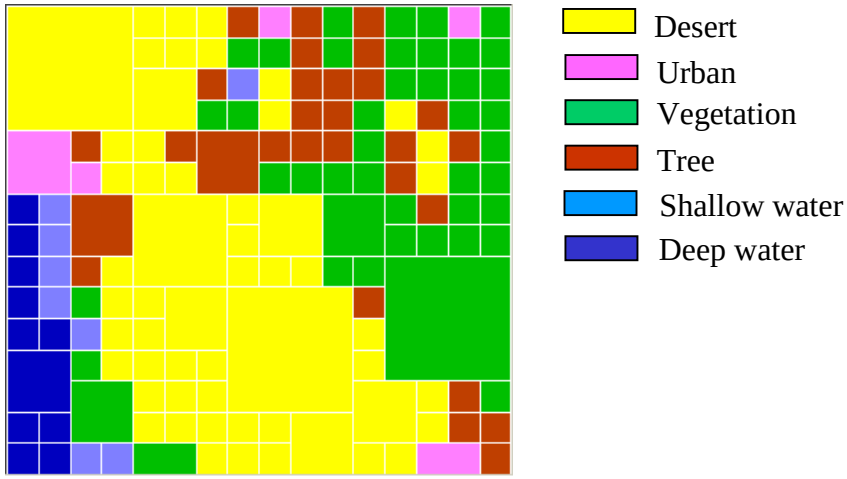

Fig. (6) Classification of the Ramadi image.

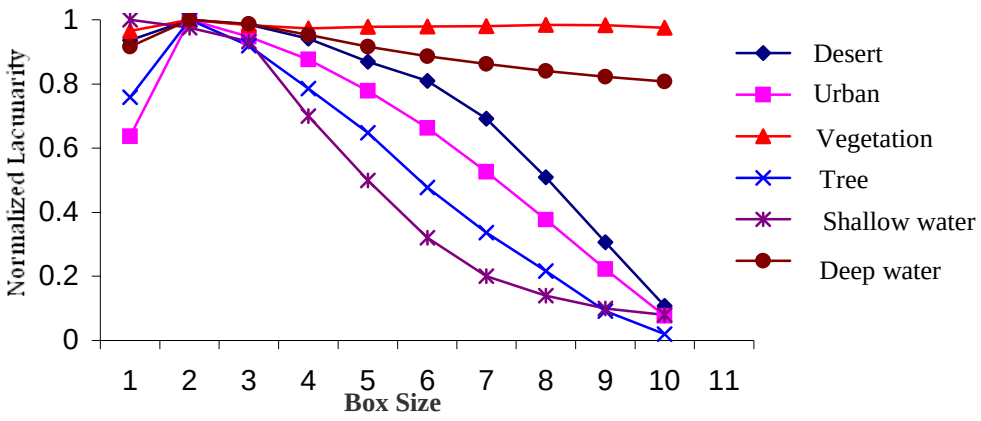

Fig. (7) Normalized lacunarity shapes of the six classes.

5. Discussion and Conclusions

The extraction of the lacunarity by using box counting method necessitate to make the sliding window is large enough (i.e. 10×10 pixels at least). But this restriction is slightly confusing the segmentation results. Where, the segmented blocks not appeared totally spectral uniform. Thus the resulted lacunarity shapes belong to the same class have small differences in between, while the lacunarities of different classes showed different shapes in comparison with each other. The resulting lacunarity curves gave an impress about the stability of the general shape of the lacunarity belong to the same class in the image. Actually, smaller S_{ij} made the number of classes greater than six classes, this problem was passed by finding the class of fewer members and distribute these members along other closest classes, this is done by making the other classes accepting greater distorted lacunarities (i.e., less S_{ij}). This process can be repeated if the number of classes was maintained greater than six.

Practically, it is found that 90% is the actual percentage of the information available in the first PC. But when it was sliding into higher or lower value, the classification result in both cases was not same. The total percentage of classification was decreased greatly by decreasing the contribution weight of the first PC, and it increased lightly by increasing the contribution weight of the first PC even it became in saturation state at/after the nineties percentages. Fig.(8) describes the dependency of the classifier efficiency on the contribution weight of the first PC. Such result indicates that the classifier depends basically on the first PC. Thus the total classification percentage can be only driven by using the first PC. This ensure that the KL transform strengthen the relation between the classifier and the first PC that carried the most information of the image with account of other PC′s.

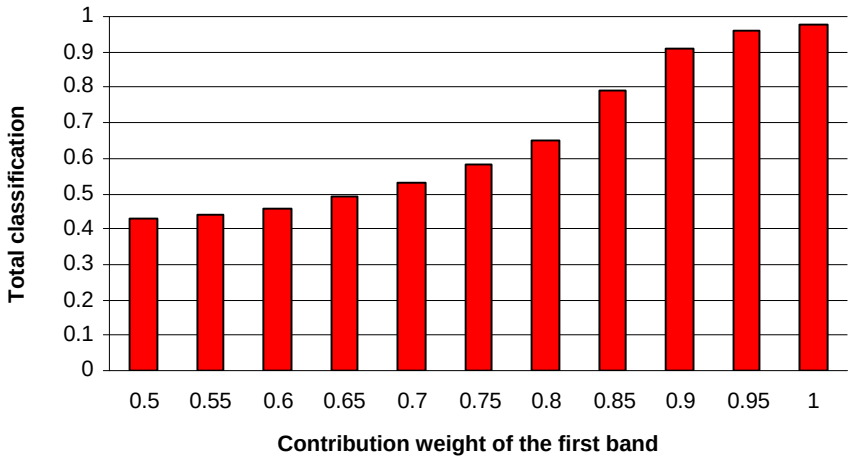

Fig. (8) Total classification percentage versus contribution weight of the first PC.

In general, the fractal analyses applied on multibands satellite image showed good classification results. One can note that the fractal technique is sensitive to the image contrast through specific resolution. In the same time, the box counting method restricts the quadtree segmentation by dictating large block size. Also, the results showed few percent of confused lacunarity because its shape appears similar to that of two approached classes, so an interference occurred between two different classes. This is the reason of making the total classification percentage is not full.

6. Conclusions and Further work

The promising results of classification tell that the fractal description exhibit the satellite images since it was effective in classifying different spectral details of subimage. Moreover, the adopted lacunarity was a successful parameter since it gave acceptable results in the classification task. As future work, one can analytically studying the effect of the similarity measure distribution on the

الخلاصة

في هذا البحث تم استخدام صورة أقمار صناعية بستة حزم ذات مناطق تجريب معروفة. إن الطريقة المعتمدة في التصنيف تتبنى تحويل الحزم الستة باستخدام تحويل KL. إن توزيع المعلومات الصورية للحزم المحولة يتركز في الحزمة الأولى و يتناقص تدريجيا حتى الحزمة الأخيرة. لذلك يمكن استخدام الحزم الثلاثة الأولى التي تحمل معظم معلومات الصورة للحصول على تصنيف أدق. كل حزمة من الحزم الثلاثة قطعت إلى مقاطع بطريقة الشجرة الرباعية (Quadtree) بشروط مقترحة جديدة. ومن ثم حسب المصنف الفجوة (Lacunarity) الكسوري المعروف لكل مقطع لاجل تصنيفها. النتائج بينت ستة أصناف واضحة في الصورة. وقد كانت نسبة التصنيف الكلية بحدود 91% عندما تشارك الحزمة الأولى بمقدار 90%، وهذه النسبة تزداد زيادة طفيفة بزيادة مقدار مشاركة الحزمة الأولى.

result of classification percentage. Also, one can classify the image without KL transforms and compare its result with that of the current research in terms of their fastness and accuracy.

7. References

[1] Kannappan P. and Feng Z., "Automatic Land Cover Classification Using Evolutionary Algorithms and Decision Trees", Proceeding of IIC, August 21-25 2000, pp. 36-45.

[2] Kushima K. and Masashi Y., "Integrating Hierarchical classification and Content-based Image Retrieval", Proceeding of ICCP, August 21-25 2000, pp. 109-123.

[3] Jain A. K., "A Fast Karhunon-Loeve Transform for Digital Restoration Degraded by White and Colored noise", IEEE, Vol. C-26, 2005, PP. 560-571.

[4] Antoni B. and Nuno V., "Probabilistic Kennels for the Classification of Auto-Regressive Visual Processing", IEEE, Conference on computer Vision and Pattern recognition, San Diago, 2005.

[5] Iodice A., Migliaccio M., and Riccio D., "SAR Imagery Classification: The Fractal Approach", Proceeding, Europto Series, Vol. 936, 1995, pp. 539-551.

[6] Walsh T. R. "Efficient Axis-Translation of Binary Digital Pictures", Computer vision and image processing, Vol. 41, 1991, pp. 282-292.

[7] Desachy J., 1994, "Image and Signal Processing for Remote Sensing", Proceeding, Europto Series, Vol. 2315, pp.539-551.

[8] Keller J. M. and Cken S., 1989, "Texture Description and Segmentation through Fractal Geometry" Computer vision and image processing, Vol. 45, pp. 150-166,

[9] Auson L. F. 1993, "Fractal Image Compresion", Byte, pp.195-202.

[10] Keller J. M., Cronover R. M., and Chen R. Y., 1987, "Characteristics of Natural Scenes Related to Fractal Dimension", IEEE, Transaction on pattern analysis and machine intelligence, Vol. PAMI-9, No.5, pp.621-627.